Sensing and Fingerprinting of Ultra-Wide Band Radio in UCELLS project

Roberto LLORENTE[1], Maria MORANT[1], Jonathan DUPLICY[2], Toon VAN WATERSCHOOT[3], Vincent LE NIR[3], Marc MOONEN[3], José PUCHE[4] and Jac ROMME[5]
[1] Universidad Politécnica de Valencia, C/ Camino de Vera, S/N, 46022, Valencia, Spain
Tel: +34 96 3879768, Fax: +34 96 3877827, Email: rllorent@ntc.upv.es
[2]Agilent Measurement Research Laboratory, Wingepark 51, 3110, Rotselaar, Belgium
Tel: +32 1646 97 94, Fax: +32 1644 54 81, Email: jonathan_duplicy@agilent.be
[3] Katholieke Universiteit Leuven, ESAT-SCD, Kasteelpark Arenberg 10, 3001 Leuven, Belgium
Tel: +32 1632 19 27, Fax: +32 1632 19 70, Email: toon.vanwaterschoot@esat.kuleuven.be
[4]DAS Photonics S.L, Camino de Vera s/n, Building 8F, 46022 Valencia, Spain
Tel: +34 96 3556150, Fax: +34 96 3562581, Email: jpuche@dasphotonics.com
[5]IMST GmbH, Kamp-Lintfort NRW, Germany
Tel: +49 2842 981 0, Fax: +49 2842 981 199, Email: romme@imst.de

Abstract: This paper reports the experimental work performed in the framework of the ICT-1-216785 UCELLS project aiming at sensing ultra-wideband radio signals and their fingerprinting for cognitive radio management purposes. The experimental results demonstrate the successful capture and processing of UWB radio signals employing a photonic analog-to-digital converter. This approach permits both to cover a large frequency span without filtering and down-conversion stages altogether an excellent sensibility due to the engineering of the signal amplification stages through the optical and electronics domains. The experimental work herein reported demonstrates that -48 dBm peak levels can be sensed with 11.2 dB SNR using the proposed photonics technique. This technique enables the precise fingerprinting of the UWB transmitters in the area. Successful operation has been also demonstrated detecting the time frequency hopping of UWB transmissions captured and processed by the photonic analog-to-digital converter. The experimental results confirm the excellent performance of the fingerprinting algorithms identifying the presence of signal in each band of the frequency hopping and the silence periods. The identification of these transmission parameters enables cognitive management of the different transmitters maximizing the overall system capacity.

Keywords: Cognitive radio, photonic analog to digital converter, fingerprinting, sensing.

1. Introduction

Due to their efficient usage of the spectrum, Cognitive Radio (CR) technologies are expected to be a key solution to the foreseen spectrum scarcity problem due to the ever increasing number of subscribers and data rates. CR systems rely on first getting the knowledge of the radio environment (sensing stage). The data are then processed and used to maximize the user capacity and to mitigate the possible interference between sharing applications by adapting the transmission parameters [1]. Interference mitigation is expected to be inherent to present and future wireless transmission standards by the inclusion of detect-and-avoid functionalities. This is the case, by example, of the support of detect-and-avoid techniques in recent regulation related to ultra-wideband radio [2]. The present paper focus on the sensing stage and associated fingerprinting targeted to Ultra-Wideband (UWB) signal.

Sensing radio signals is a challenging task when both a large bandwidth and high sensitivity must be achieved. Radio measurement in a large frequency span is typically done using a spectrum analyser and a frequency down-conversion stage sweeping the desired frequency range. The spectrum analyser is synchronized with a sampling digitizer in order to capture the entire spectrum. These techniques become more complex and expensive as the power of the sensed signals decreases and as their frequency range increases. Unfortunately, UWB, our focus in this article, is characterized by its very low power and very high bandwidth. Indeed, its frequency occupancy spans from 3.1 until 10.6 GHz and its expected power spectral density ranges from -41.3 to -65.3 dBm/MHz [3]. Photonic analog-to-digital converters (Ph-ADC) have been proposed as a suitable technique capable of dealing with such power levels, known as ultra-low power radio, achieving more than 20 dB signal-to-noise ratio with an RF carrier input of -65 dBm [4].

Several Ph-ADC architectures have been reported in the state-of-the-art in order to improve the conventional electronic ADCs (E-ADC) performance by using photonic techniques [5]. In this paper, a time-stretched Ph-ADC architecture [6] with engineered optical and electrical amplification is proposed to detect UWB signals. The captured data is further processed for fingerprinting applications. These results have been obtained inside the FP7 European project "UCELLS" for ultra-wide band real-time interference monitoring and cellular management strategies [7].

The paper is organized as follows: Section II presents a brief description of cognitive radio systems. Section III describes the spectrum sensing approach proposed by UCELLS project. Section VI explains the fingerprinting algorithms used in the proof-of-concept, and Section V presents the experimental validation of the proposed technique. Finally, Section VI summarizes the conclusions from this work.

2. Photonics-enabled Cognitive Radio

Figure 1 shows an example of application scenario where cognitive radio techniques could be applied. In this scenario a set of transmitters are placed in a given area forming different cells. The UWB picocell cluster concept was presented in [8]. In this case, the transmitters are emitting at very low power levels, also called ultra-low power radio [9], i.e. UWB signals that cover the band from 3.1 to 10.6 GHz with very low power levels. In the proposed system, several sensors are placed along a given area to detect the radio signal present in the environment and connected to a centralized unit where the detected signals are processed to decide the management command to change the transmission parameters of the devices.

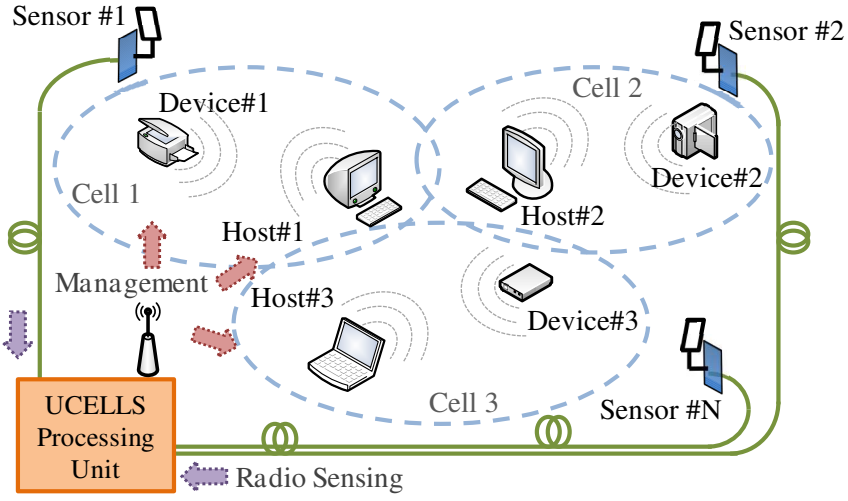

Figure 1: Mean features of the cognitive radio system in an application scenario

The system depicted in Figure 1 aims to identify portions of spectrum that are unused and to share that spectrum without interfering with the existing users transmitting in the area. In order to achieve this, the cognitive radio system should have detailed information concerning its environment and employ this information to decide on its transmission behaviour. Basically, they cognitive radio system needs to perform three main activities:

1. Obtain complete information of the operational radio environment and the location of the transmitters present in the area
2. Process this environment information and decide on the gathered information
3. Adapt and change the transmission characteristics (in this case: frequency channel and transmission power level of each host/device) based on this decision

As can be observed in Figure 1, in order to adapt the communication parameters of the transmitters, some radio information needs to be processed in the central unit. This processing is based on the active monitoring of several factors in the external and internal radio environment detected by the sensors along the area.

A real time spectrum monitoring technique based on photonic analog-to-digital conversion has been proposed in the European project UCELLS. This photonic analog-to-digital converter architecture is used to stretch the radio signals detected by the sensors and reduce the frequency range needed to be processed.

The management strategy proposed in UCELLS can be summarized as: the access nodes capture the signal to monitor the used spectrum to centrally control the UWB channel employed and the maximum transmitted power of each transmitter shown in Figure 1. An example of a conventional spectrum before and after applying cognitive radio techniques is shown in Figure 2. In this paper a proof of concept of the sensing architecture of UWB signals and the fingerprinting processing developed inside UCELLS project are presented.

3. Sensing UWB radio

In the European project FP7-ICT-1-216785 "UCELLS", a picocell clustering technique has been proposed for extending the UWB radio range in application scenarios of medium range, i.e. home environments or small offices [8]. In order to use the picocell cluster architecture depicted in Figure 1, it is necessary to guarantee that there is no interference between the different cells. Moreover, the spectrum usage should be maximized when a large number of transmitters is present in a given area. These aims can be achieved by including power-flow control techniques and spectrum monitoring in the area of operation.

As discussed previously, the very wide UWB frequency range (from 3.1 to 10.6 GHz) makes sensing very challenging. The conventional electronic ADC sensibility is in this case too limited for monitoring due to the low power levels compared with other licensed/unlicensed services using higher power transmission levels.

To be able to cope with both wide bandwidth and very low power signals, a Ph-ADC architecture (including engineered optical and electrical amplification) was proposed in the framework of the UCELLS project. Moreover, this technique can be used for cognitive radio management strategies as it increase the sensibility and the bandwidth of electronic ADC for wideband spectral monitoring and detect signals with very low power level.

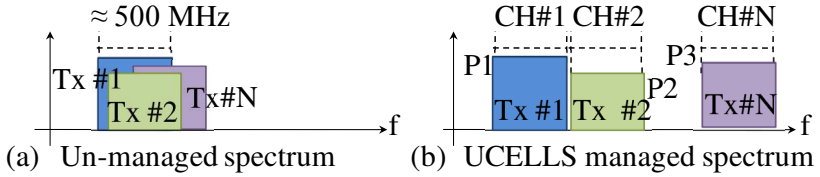

Figure 2: (a) Electrical spectrum of a given area without cognitive radio management and (b) proposed resulting spectrum after UCELLS management

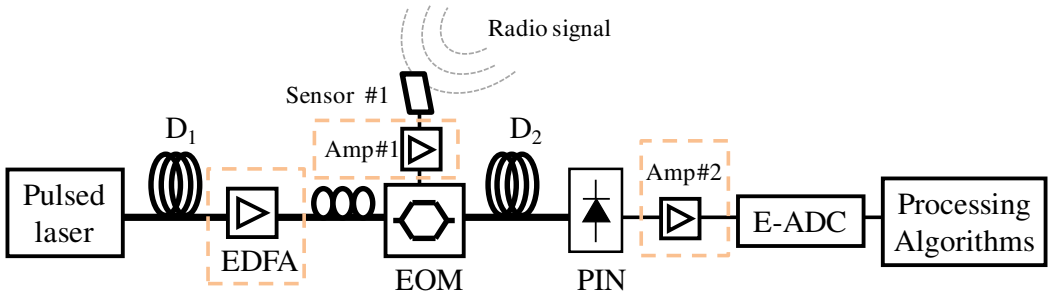

Figure 3: Proposed single-channel Ph-ADC architecture with engineered optical and electrical amplification.

The single-channel Ph-ADC architecture, shown in Figure 3, was reported in [10] and its operation can be summarized as follows. A pulsed laser source generates optical pulses that are transmitted through a first spool of fiber with high chromatic dispersion value. The accumulated chromatic dispersion of this first spool of fibre (D_1) converts the spectral components of the optical source to time domain in a λ-to-t mapping process. A segment of the radio signal captured by the sensor antenna is modulated using an electro-optical modulator. The modulated signal is propagated in a second spool of fibre with total dispersion D_2 to finish the conversion. After photodetection and amplification, the signal is stretched in time and its spectrum appears compressed by the stretching factor defined as the relation between the chromatic dispersion of the second and the first spools of fiber $M = D_2/D_1$.

An optical amplification stage is included before the electro-optical modulator (EOM) to compensate the optical losses of the high dispersive fibers (D_1 and D_2). In addition, engineered electrical amplification is included in the system in two stages: the first one located at the sensor after the receiver antenna and before the EOM input, and the second one after the PIN photodetector as displayed on the Figure 3.

4. Fingerprinting processing

The role of fingerprinting is to give out an accurate image of the actual radio activity captured by the set of sensors. While the information from several sensors is required to perform (3D) source localization, only one sensor is necessary to perform the fingerprinting task. In practice, fingerprinting is applied to each sensor separately but the results of different sensors could be merged to enhance the accuracy.

A two-step approach has been taken to address the UWB fingerprinting task. A coarse analysis is done using a periodogram, in a second stage, the time domain structure of the signal is used to enhance the first estimation. These two steps are detailed hereafter.

As first step, an averaged periodogram is computed to give an estimate of the power spectral density (PSD) of the received sequence:

$$S_{avg} = \frac{1}{M} \sum_{m=0}^{M-1} \left| FFT\left(y_m \right) \right|^2 \quad (1)$$

An averaged estimation for each UWB frequency band is computed and compared with the noise levels. This gives a first estimation about the presence or the absence of UWB signal. The signal is then downconverted to baseband per UWB frequency band basis and sent to the second stage.

Usually, OFDM modulation is used with a cyclic prefix to mitigate multipath. Classically, applying a time domain correlation will reveal the structure by exhibiting correlation peaks. In the case of ECMA-368 [11] UWB, zero-padding is used in place of the cyclic prefix.

This time-domain structure can be seen later in the experimental results shown in Figure 7. It is clear that in this case, a correlation will fail to reveal the signal structure. Instead, we have proposed a new power correlation feature given by [12]:

$$d(k) \overset{\Delta}{=} \frac{1}{N}\sum_{i=0}^{N-1} |y(i)|^2 |y(i-k)|^2 \quad k \in [0K\ N-1] \tag{2}$$

with y the received signal. As illustrated by Figure 4, d is characterized by a train of triangle pulses with period equal to the symbol duration.

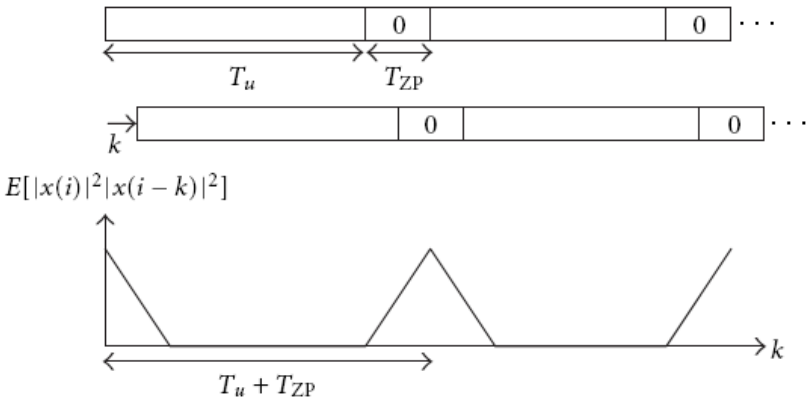

Figure 4: Power correlation on ZP-OFDM

The time duration between peaks is estimated and put in perspective with the known a-priori symbol duration. A match will confirm the presence of an UWB signal. For further details including the effect of multipath, we refer the reader to [12].

5. Experimental Setup and Results

Figure 5 describes the experimental setup used for the proof-of-concept of UWB radio sensing and fingerprinting processing using the proposed Ph-ADC architecture in a single channel configuration. The pulsed laser (Pritel femtosecond fiber laser) generates optical pulses of ≈ 1.6 ps width with 3.233 MHz repetition rate.

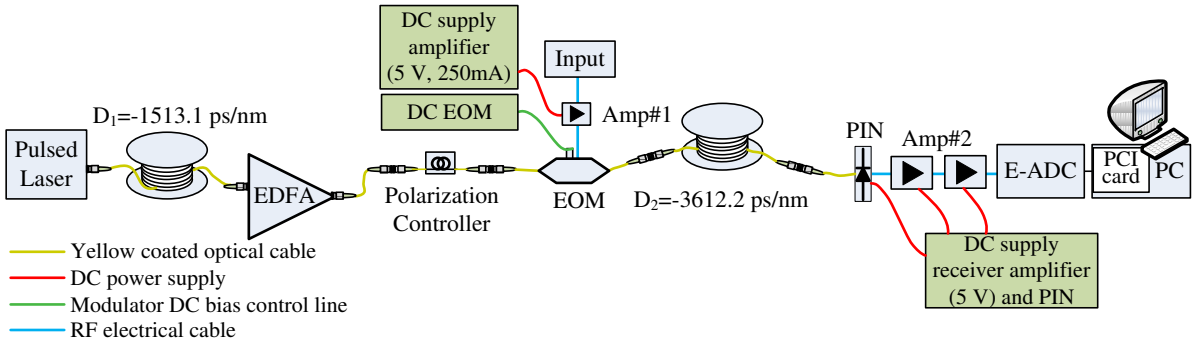

Figure 5: Experimental proof-of-concept setup of a single-channel Ph-ADC architecture with engineered optical and electrical amplification for UWB sensing and fingerprinting processing

The dispersion compensating fibres used in the laboratory proof-of-concept are two low loss dispersion slope compensating modules from OFS (LLMicroDK) with dispersion D_1= -1513.1 ps/nm and D_2=-3612.2 ps/nm respectively, what leads to a stretching factor of $M \approx 3.4$. The optical amplifier is an EDFA (Exelite XLT-SFA-19) with 19 dBm saturated power and 4.5 dB noise figure. The antenna amplifier (Amp#1) is a low noise amplifier with 42 dB gain manufactured by DAS Photonics. The EOM is a Mach-Zehnder modulator (Photline MX-LN-10) with V_π=3.8 V. The PIN photodetector (XPDV2020R) has 0.65 A/W responsivity. The receiver amplifier (Amp#2) contains two amplification stages with 62 dB total gain and a high pass filter with 800 MHz cut-off frequency.

The stretched signal is digitized by an electrical ADC (E-ADC) and processed. The core of the E-ADC is an Agilent Acqiris DC282 board with a 2 GHz front-end and a 10-bit sampling rate at 8GS/s [13]. The UWB signal located in the 3 first frequency bands (from 3.168 GHz to 4.752 GHz that are commercially available nowadays) after the time stretching of M=3.4 will be approximately 1.75 GHz, which fits with the 2 GHz front-end specification of the E-ADC.

In first place, the input of the single-channel Ph-ADC is feed with a carrier (generated with Agilent E4438) of centre frequency 3.4 GHz and -48 dBm peak power. The received electrical spectrum of the tone signal after the single-channel Ph-ADC is shown in Figure 6(a). The power spectral density is estimated using the periodogram as shown in Figure 6(b). In this figure it can be observed the main lobe in 1 GHz (=3.4 GHz peak / M) and several side lobes. From these figures it can be observed that the signal to noise ratio (SNR) is approximately 11.2 dB.

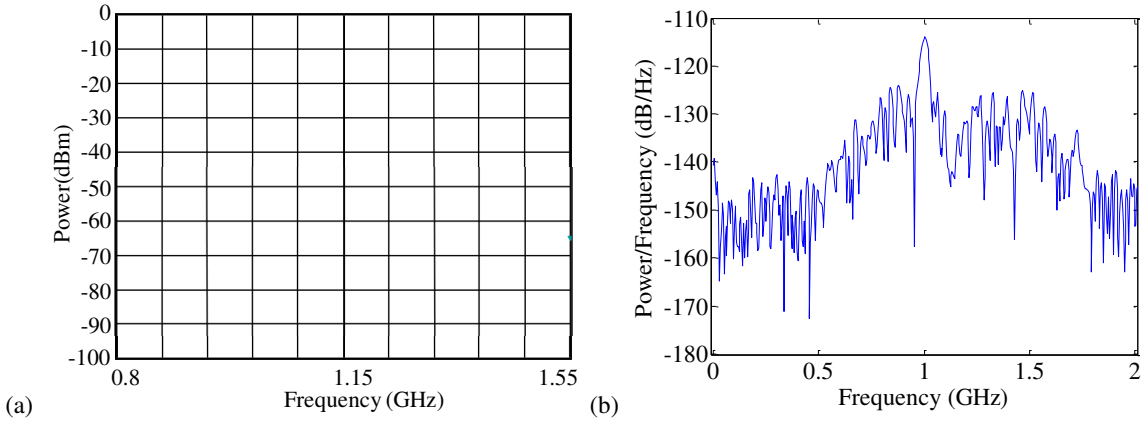

Figure 6: (a) Received electrical spectrum with an input tone at 3.4 GHz (RWB= 50 kHz) and (b) power spectral density estimate via periodogram

Then, the Ph-ADC performance for sensing UWB signals is studied. The UWB signal is generated (Input generator in Figure 5) with a Wisair dongle connected directly to the antenna amplifier (Amp#1). This UWB dongle generates a fully-compliant ECMA-368 standard [11] UWB signal. In this case, we configured a bitrate of 480 Mbit/s with time frequency code configuration TFC1 (frequency band pattern 1,2,3,1,2,3), and a transmission power -20 dB under the regulatory threshold. Figure 7 shows the captured time signal after the Ph-ADC architecture with UWB input signal using time frequency code TFC1.

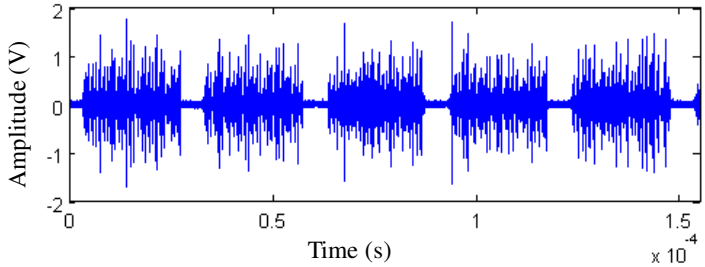

Figure 7: Captured time signal after photonic ADC when transmitting UWB TFC1 configuration

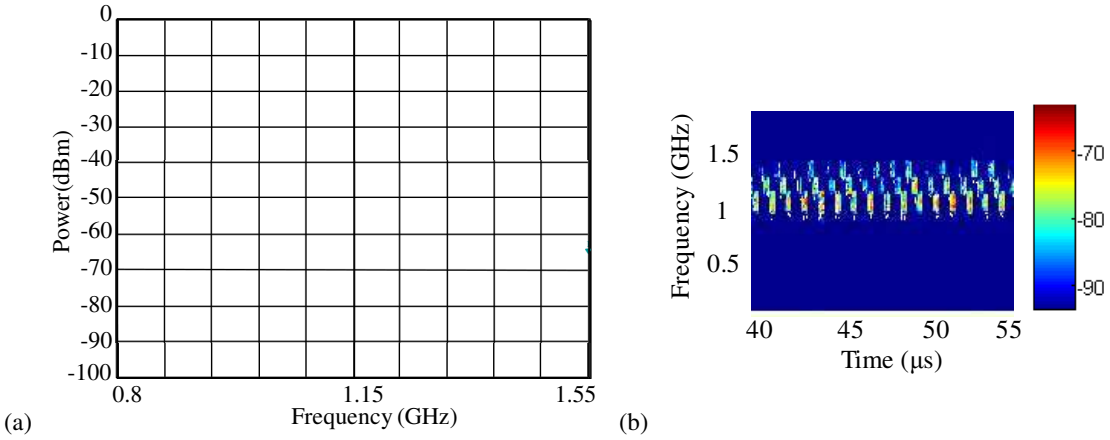

Figure 8: (a) Received electrical spectrum (RWB=50 kHz) and (b) processed spectrogram of the received UWB signal using TFC1 configuration after the single-channel photonic-ADC architecture

The time stretching is confirmed too observing the spectrum at the output of the system shown in Figure 8, where the first UWB band from 3.1 to 4.8 GHz is reduced to 0.91 to 1.41 GHz after the time stretching architecture with M=3.4. This can be seen too in the processed spectrogram shown in Figure 8(b). If we analyze further the results looking at the power levels shown in Figure 8, there is a difference between the first UWB frequency (0.91 GHz) and the last one (1.41 GHz) of approximately 8 dB. This effect is mainly due to the amplifier stages but also the modulator and cables response. For example, the antenna amplifier (Amp#1 in Figure 5) manufactured by DAS Photonics has a non-uniform gain response in the whole UWB band. For the first three channels under study, the amplifier gain is G=44.9 dB for the lowest UWB frequency and G=38.4 dB for the highest which is a difference of 6.5 dB. This should be improved in order to minimize the power level difference between each UWB band.

Activating the fingerprinting algorithm, the software starts processing the retrieved data from the E-ADC and locates the UWB spectral power in each band for each time slot. An example of the fingerprinting processing output is shown in Figure 9.

Starting to analyze the data

Time1: 8.718050e-002μs	67.3dB	-100dB	-100dB	Time40: 1.214879e+001μs	63.5dB	-100dB	-100dB
Time2: 3.964525e-001μs	-100dB	65.9dB	-100dB	Time41: 1.245806e+001μs	-100dB	69dB	-100dB
Time3: 7.057244e-001μs	-100dB	-100dB	65.1dB	Time42: 1.276733e+001μs	-100dB	-100dB	66.5dB
Time4: 1.014996e+000μs	73.6dB	-100dB	-100dB	Time43: 1.307660e+001μs	67.5dB	-100dB	-100dB
Time5: 1.324268e+000μs	-100dB	67.6dB	-100dB	Time44: 1.338588e+001μs	-100dB	67.6dB	-100dB
Time6: 1.633540e+000μs	-100dB	-100dB	49dB	Time45: 1.369515e+001μs	-100dB	-100dB	66.2dB
Time7: 1.942812e+000μs	67.6dB	-100dB	-100dB	Time46: 1.400442e+001μs	80.5dB	-100dB	-100dB
Time8: 2.252084e+000μs	-100dB	65dB	-100dB	Time47: 1.431369e+001μs	-100dB	74.2dB	-100dB
Time9: 2.561356e+000μs	-100dB	-100dB	57.1dB	Time48: 1.462296e+001μs	-100dB	-100dB	65.1dB
Time10: 2.870628e+000μs	62.4dB	-100dB	-100dB	Time49: 1.493224e+001μs	64.5dB	-100dB	-100dB
Time11: 3.179900e+000μs	-100dB	72.1dB	-100dB	Time50: 1.524151e+001μs	-100dB	68.1dB	-100dB
Time12: 3.489172e+000μs	-100dB	-100dB	59.9dB	Time51: 1.555078e+001μs	-100dB	-100dB	62.8dB
Time13: 3.798444e+000μs	74.7dB	-100dB	-100dB	Time52: 1.586005e+001μs	75dB	-100dB	-100dB
Time14: 4.107716e+000μs	-100dB	72.3dB	-100dB	Time53: 1.616932e+001μs	-100dB	66.6dB	-100dB
Time15: 4.416988e+000μs	-100dB	-100dB	58.9dB	Time54: 1.647860e+001μs	-100dB	-100dB	60dB
Time16: 4.726260e+000μs	72.9dB	-100dB	-100dB	Time55: 1.678787e+001μs	69dB	-100dB	-100dB
Time17: 5.035532e+000μs	-100dB	69.4dB	-100dB	Time56: 1.709714e+001μs	-100dB	68.5dB	-100dB
Time18: 5.344804e+000μs	-100dB	-100dB	64.3dB	Time57: 1.740641e+001μs	-100dB	-100dB	57.1dB
Time19: 5.654076e+000μs	-100dB	-100dB	-100dB	Time58: 1.771568e+001μs	60.6dB	-100dB	-100dB
Time20: 5.963348e+000μs	-100dB	-100dB	-100dB	Time59: 1.802495e+001μs	-100dB	56.9dB	-100dB
Time21: 6.272620e+000μs	-100dB	-100dB	-100dB	Time60: 1.833423e+001μs	-100dB	-100dB	56dB
Time22: 6.581892e+000μs	-100dB	-100dB	-100dB	Time61: 1.864350e+001μs	78.6dB	-100dB	-100dB
Time23: 6.891164e+000μs	-100dB	-100dB	-100dB	Time62: 1.895277e+001μs	-100dB	71.2dB	-100dB
Time24: 7.200436e+000μs	-100dB	-100dB	-100dB	Time63: 1.926204e+001μs	-100dB	-100dB	57.9dB
Time25: 7.509708e+000μs	-100dB	-100dB	-100dB	Time64: 1.957131e+001μs	64.4dB	-100dB	-100dB
Time26: 7.818980e+000μs	-100dB	-100dB	-100dB	Time65: 1.988059e+001μs	-100dB	54.2dB	-100dB
Time27: 8.128252e+000μs	-100dB	-100dB	-100dB	Time66: 2.018986e+001μs	-100dB	-100dB	62.5dB
Time28: 8.437524e+000μs	-100dB	-100dB	-100dB	Time67: 2.049913e+001μs	54.7dB	-100dB	-100dB
Time29: 8.746796e+000μs	-100dB	-100dB	-100dB	Time68: 2.080840e+001μs	-100dB	51.9dB	-100dB
Time30: 9.056068e+000μs	-100dB	-100dB	-100dB	Time69: 2.111767e+001μs	-100dB	-100dB	56.2dB
Time31: 9.365340e+000μs	-100dB	-100dB	-100dB	Time70: 2.142695e+001μs	72.5dB	-100dB	-100dB
Time32: 9.674612e+000μs	-100dB	-100dB	-100dB	Time71: 2.173622e+001μs	-100dB	72dB	-100dB
				Time72: 2.204549e+001μs	-100dB	-100dB	66.6dB

Figure 9: Fingerprinting analysis for UWB TFC1 configuration

Figure 9 shows the fingerprinting of a TFC1 transmission, with the hopping pattern 1,2,3,1,2,3. The time runs in the vertical, and each of the three data columns represents each of the three first frequency bands in UWB.

The -100 dB labels indicate that no OFDM UWB symbols were detected in that time slot at that frequency band. If the number is different, then transmission presence was detected. In the example of Figure 9, the frequency hopping pattern is clearly identifiable. Furthermore, the silent period in the middle, between Time19 and Time32, appears as an absence of any OFDM as can be confirmed in the time signal shown in Figure 7.

6. Conclusions

The experimental results in this proof-of-concept experiment indicate that the proposed Ph-ADC technology is a suitable approach for sensing ultra-low power UWB radio signals in real-time. The experimental set-up permits the sensing -48 dBm sensibility and with 11.2 dB SNR. This SNR successfully enables the adequate fingerprinting of the UWB signals detected.

The fingerprinting applied to the sampled data consists in, first, computing an averaged periodogram to give an estimate of the power spectral density of the received sequence, and second, a time domain correlation will confirm the presence of an UWB signal.

The results of the fingerprinting process of the received signal in a single-channel Ph-ADC architecture with UWB input signal using frequency hopping were presented and analyzed. The processing algorithms were able to detect the transmission presence in each band of the frequency hopping and the silent periods.

Acknowledgments

This work has been partly funded by the European Union through the FP7-ICT-216785 UCELLS project. The NoE FP7-ICT-216863 BONE is also acknowledged. Maria Morant's work is supported by Spain FPU MEC grant AP2007-01413.

References

[1] J. Mitola III and G. Q. Maguire, "Cognitive Radio: Making Software Radios More Personal", IEEE Personal Communications, Vol. 6, Issue 4, pp. 13-18, Aug 1999.

[2] ETSI TS 102 754 V1.1.1: "Electromagnetic compatibility and Radio spectrum Matters (ERM); Short Range Devices (SRD); Technical characteristics of Detect-And-Avoid (DAA) mitigation techniques for SRD equipment using Ultra Wideband (UWB) technology", June 2008.

[3] FCC 02-48: "Revision of part 15 of the commission's rules regarding ultra-wideband transmission systems", FCC, April 2002.

[4] R. Llorente, M. Morant, J. Puche, J. Romme and T. Alves, "Sensing Ultra-Low-Power Radio Signals by Photonic Analog-to-Digital Conversion", 35th European Conference on Optical Communication ECOC2009, Vienna, Austria, 20-24 September 2009.

[5] A.S. Bhushan, et al., "130-GSa/s photonic analog-to-digital converter with time stretch preprocessor", IEEE Photonics Technology Letters, Vol. 14, Issue 5, pp. 684-484, May 2002.

[6] Y. Han, B. Jalali, "Photonic time-stretched analog-to-digital converter: fundamental concepts and practical considerations", Journal of Lightwave Technology, Vol. 21. Issue 12, pp. 3085- 3103, December 2003.

[7] FP7-2007-IST-1-216785 Ultra-wide band real-time interference monitoring and CELLular management Strategies, http://www.ist-ucells.org

[8] R. Llorente, et al. "Management of UWB Picocell Clusters: UCELLS Project Approach", invited paper in 2008 IEEE International Conference on Ultra-Wideband, ICUWB2008, Vol. 3, pp. 139-142, September 2008.

[9] J. R. Long, et al., "Energy-efficient Wireless Front-end Concepts for Ultra Lower Power Radio", IEEE 2008 Custom Intergrated Circuits Conference (CICC), pp. 587-590, 2008.

[10] R. Llorente, M. Morant, J. Puche, T. Alves and J. Romme "Cognitive Radio by Photonic Analog-to-Digital Conversion Sensing", Second International Workshop on Cross-Layer Desing, IWCLD2009, Spain, June, 2009.

[11] ECMA-368: "High rate ultra wideband PHY and MAC Standard", ECMA International Standard, Dec. 2007.

[12] V. Le Nir, T. van Waterschoot, M. Moonen and J. Duplicy, "Spectral monitoring and parameter estimation for ZP-OFDM signals,'' Proc. 17th European Signal Process. Conf. (EUSIPCO '09), Glasgow, UK, Aug 2009.

[13] Agilent U1065A Acqiris 10-bit High-Speed cPCI Digitizers. Information available at the website: http://www.home.agilent.com/agilent/product.jspx?nid=-35502.733409.00&cc=US&lc=eng